The International Journal of Advanced Manufacturing Technology

Investigation of solution acidity influence on the morphological structure, physical and mechanical properties of particles reinforced tungsten alloys

--Manuscript Draft--

Manuscript Number:	JAMT-D-20-03191R1
Full Title:	Investigation of solution acidity influence on the morphological structure, physical and mechanical properties of particles reinforced tungsten alloys
Article Type:	Original Research
Keywords:	Particle reinforced tungsten alloy; Doping zirconia; Yttria - stabilized zirconia; mechanical property.
Corresponding Author:	Fangnao Xiao Femto-st Institute Besancon, FRANCE
Corresponding Author Secondary Information:	
Corresponding Author's Institution:	Femto-st Institute
Corresponding Author's Secondary Institution:	
First Author:	Fangnao Xiao
First Author Secondary Information:	
Order of Authors:	Fangnao Xiao
	Thierry Barriere
	Gang Cheng
	Qiang Miao
	Shiwei Zuo
	Shizhong Wei
	Liujie Xu
Order of Authors Secondary Information:	
Funding Information:	National Natural Science Foundation of China (U2004180) — Prof. Liujie Xu National Natural Science Foundation of China (51874185) — Prof. Qiang Miao Nanjing university of aeronautics and astronautics PhD short-term visiting scholar project (190107DF06) — Mr. Fangnao Xiao
Abstract:	Yttria - stabilized zirconia particles reinforced tungsten alloys were fabricated by using azeotropic distillation process coupled with powder metallurgy techniques. The influence of pH value of the original solution on the precursor powders' morphology, wear and mechanical properties of alloys were deeply studied. It showed that the precursor' powder synthesized under solution with pH of 2 possesses finer particles' size. The grain sizes of tungsten reinforced alloys obtained with different pH values varies from 2 to 6 μm, extremely smaller than that of pure tungsten. When pH value increases from 2 to 8, more and more bonding zirconia particles are obtained. The reinforced tungsten alloy prepared based on the solution of pH equal to 2 have a better morphological and mechanical properties than the other two alloys prepared based on the solution of pH values of 5 and 8, respectively. The wear resistance of the reinforced tungsten alloy increases firstly, then decreases with the doping amount of zirconia

	particles. It is confirmed that the pH 2 value and chemical composition of the tungsten alloy with 3.0 wt. % Zr(Y)O 2 exhibits the best wear resistance. The mechanical properties of the particle reinforced tungsten alloy are improved with the decrease of pH value. The ultimate compressive strength and ultimate strain value of pH 2 reach to 1009 MPa and 0.23, respectively. The evolution of the relative density and associated porosity increases with the pH value. The abrasion mechanism was analyzed in detail.

Response to Editor and Reviewer Comments:

Ref. No.: JAMT-D-20-03191

Title: Investigation of solution acidity influence on the morphological structure, physical and mechanical properties of particles reinforced tungsten alloys.

We greatly appreciate the work of the editor and the referees in reviewing this manuscript. We have addressed the issue indicated in the review reports. The suggestion of the reviewer has been taken into account in the revised manuscript. The improvement of the revision is marked in red.

Reviewer #2: In this work, the yttria - stabilized zirconia particles (Zr(Y)O2) strengthened tungsten alloys (W-Zr(Y)O2) were developed via azeotropic distillation method combined with powder metallurgy techniques, but the content of the present work is not new. It is well known that the wear resistance of W-Zr(Y)O2 alloy has been widely reported. The results in this work are not enough, which can not attract the readers of JAMT. In addition, the manuscript is also not well prepared.

Response: We have improved the manuscript by taking into account your comments. We have added new contents on the porosity, mechanical property and wear resistance of the reinforced W alloys in function of pH value. The revised manuscript is enriched and the quality of the paper is enhanced. We think it is now suitable to be published in JAMT.

Reviewer #4: The following remarks seek careful consideration while revising the manuscript. The paper is returned with minor-modification decision to the authors according to the following comments:

Thanks for your excellent work to improve the quality of this paper. Your comments were carefully considered and some modifications were added in this revised manuscript.

(1) The English language of the paper must be carefully polished before any proceeds

with the publication. There are still many typo and syntax errors remained and here some examples are presented; however, the errors in the whole text is not listed below:

--then decreases with increase in the doping amount of Zr(Y)O2. It is confirmed that the =>then decreases with an increase in the doping amount of Zr(Y)O2. It is confirmed that the

--exhibits the highest wear resistance. The abrasion mechanism was analysed in details. => exhibits the highest wear resistance. The abrasion mechanism was analyzed in detail.

--Tungsten alloys have been widely used in the defence industry, nuclear reactor, => Tungsten alloys have been widely used in the defense industry, nuclear reactor,

--The past several years, many of liquid - liquid (L - L) methods were introduced => In the past several years, many of liquid - liquid (L - L) methods were introduced

--of precursor powders were analysed. Proper calcination process was determined => of precursor powders were analyzed. The proper calcination process was determined

Response: Thank you for pointing out the typo and syntax errors. Your comments were taking into account in the revised manuscript. Moreover, the whole article was carefully checked for spelling and format style. The revised manuscript was checked to avoid the plagiarism.

(2) To eliminate confusion on the sample fabrication, it is recommended that a separate table of sample fabrication and designation be added into the revised context. It can clearly show the types of fabricated samples with the applied parameters.

Response: Thank you for your suggestions. The preparation process of the samples, associated with the processing parameters was completely explained in the revised paper and in Fig. 1.

(3) One deficiency that existed in the text is the given evidence for each test or

experiment is not consistent with others. The authors must follow the same manner to present results in the tables and figures. If authors fabricated different samples with various parameters, the results of all must be given to the readers for better comparison and for convincing based on the given discussions.

Response: Thank you for your suggestions. In Section 2, all the tests were described, including the dimension of the specimen, the testing standard and experimental parameters. All the figures and tables were explained in detail in the text. The manuscript was carefully revised to provide a height-level description.

(4) XRD patterns for all prepared specimens must be included to show the phase transformations and to prove the claim on the grain size difference. According to the text "The grain sizes of W-Zr(Y)O2 alloys prepared with the solutions of different pH values are in the range of 2 - 6 μm, much smaller than that of pure tungsten", this is necessary.

Response: Thank you for your suggestions. The alloys prepared under pH = 2 possessed the best microstructure and were analyzed by XRD, as shown in Fig. 6. The alloys prepared under pH = 5 and 8 were not analyzed due to the poor physical properties.

(5) In the introduction part, it is recommended to add some discussion on the metal matrix composites strengthened with ceramic particles. The challenges and merits could be discussed briefly. The authors may want to review the following refs on the title:

[a] Ceramics International 39 (6), 6099-6106

[b] Ceramics International 44 (3), 3128-3133

[c] International Journal of Damage Mechanics 24 (2), 245-262

[d] Materials Science and Engineering: A 598, 162-173

Response: Thank you for your comment. These relevant references were added in the revised paper.

(6) For the reference part, it is recommended to exclude the obsolete refs and substitute newly published refs after 2010. In the meantime, the number of the reviewed refs are too limited. Expanding the reviewed list is necessary.

Response: Thank you for your comment. Some recent publications were added in the revised manuscript. The papers published before 2010 were excluded in the reference list.

(7) Expanding the discussion on the Fig. 2 results is recommendation.

Response: Some more discussions were provided according to your recommendation.

(8) Discussion on the porosity and its measurement on the different fabricated samples is recommended as well.

Response: The relative density and associated porosity versus pH value were added in the revised manuscript.

(9) Fig. 5 seems to be redundant. Just claiming based on the reference would be enough.

Response: Based on your suggestion, the fig. 5 was removed.

(10) fig. 7, the stress-strain curves showed the raw data and need to be corrected. Presenting the uncorrected data is not beneficial and somehow misleading especially in the case of elongation comparison.

Response: The curves in Fig. 7 were improved according to your suggestion. The uncorrected values were replaced, as shown in Fig. 8.

Reviewer #5: 1. please provide error bar to Figure 7. What is the experiment setup and sample dimensions of compression test?

Thanks for your comments to improve the quality of this paper. Your comments were carefully considered and some modifications were added in this revised manuscript.

Response: The error bar of strain and stress was added in the curves, as shown in Fig. 8. The experiment setup and specimen dimensions were described in Section 2 of the revised paper.

2. It would be interesting to see the effect of pH on material tensile properties as well.

Response: The elaborated specimens are too small to perform the international standard tensile test. In the future, the reinforced powders will be manufactured with industrial pilot to obtain the larger dimension specimens by SPS.

Apr. 15th 2021

To

Prof. Andrew Yeh-Ching Nee, Ph.D.

Editor-in-Chief: The International Journal of Advanced Manufacturing Technology

Dear Sir,

I am pleased to submit the revised version of our research article entitled "Investigation of solution acidity influence on the morphological structure, physical and mechanical properties of particles reinforced tungsten alloys".

The reviewers' comments are addressed in the revised manuscript and the responses are appended herewith for your reference.

We believe that the improved manuscript is now appropriate for publication in Advanced Manufacturing Technology.

This manuscript has not been published nor under consideration for publication elsewhere. We have no conflicts of interest to disclose.

Thank you for your consideration.

Investigation of solution acidity influence on the morphological structure, physical and mechanical properties of particles reinforced tungsten alloys

Fangnao Xiao [a, b], Thierry Barriere [a], Gang Cheng [c], Qiang Miao [b*], Shiwei Zuo [b], Shizhong Wei [d]*, Liujie Xu [d*]

[a] Université Bourgogne Franche-Comté, FEMTO-ST Institute, CNRS/UFC/ENSMM/UTBM, Department of Applied Mechanics, 25000 Besançon, France

[b] College of Material Science and Technology, Nanjing University of Aeronautics and Astronautics, 29 Yudao Street, Nanjing 210000, China

[c] INSA CVL, Université Tours, Université Orléans, LaMé, 3 rue de la Chocolaterie, BP 3410, 41034 Blois Cedex, France

[d] National Joint Engineering Research Center for abrasion control and molding of metal materials, Henan University of Science and Technology, Luoyang 471003, China

E-mail of Corresponding author:

miaoqiang@nuaa.edu.cn (Qiang Miao)

wsz@haust.edu.cn (Shizhong Wei)

xlj@haust.edu.cn (Liujie Xu)

Abstract: Yttria - stabilized zirconia particles reinforced tungsten alloys were fabricated by using azeotropic distillation process coupled with powder metallurgy techniques. The influence of pH value of the original solution on the precursor powders' morphology, wear and mechanical properties of alloys were deeply studied. It showed that the precursor' powder synthesized under solution with pH of 2 possesses finer particles' size. The grain sizes of tungsten reinforced alloys obtained with different pH values varies from 2 to 6 μm, extremely smaller than that of pure tungsten. When pH value increases from 2 to 8, more and more bonding zirconia particles are obtained. The reinforced tungsten alloy prepared based on the solution of pH equal to 2 have a better morphological and mechanical properties than the other two alloys prepared based on the solution of pH values of 5 and 8, respectively. The wear resistance of the reinforced tungsten alloy increases firstly, then decreases with the doping amount of zirconia particles. It is confirmed that the pH 2 value and chemical composition of the tungsten alloy with 3.0 wt. % $Zr(Y)O_2$ exhibits the best wear resistance. The mechanical properties of the particle reinforced tungsten alloy are improved with the decrease of pH value. The ultimate compressive strength and ultimate strain value of pH 2 reach to 1009 MPa and 0.23, respectively. The evolution of the relative density and associated porosity increases with the pH value. The abrasion mechanism was analyzed in detail.

Keywords: Particle reinforced tungsten alloy; Doping zirconia; Yttria - stabilized zirconia; mechanical property

Nomenclature

AMT	Ammonium metatungstate
APT	Ammonium paratungstate
DBTT	Ductile–brittle transition temperature
DSC	Differential scanning calorimeter
EDS	Electron dispersive spectroscopy

HV	Vickers hardness
HR - TEM	High - resolution transmission electron microscopy
ODS - W	Oxide particles dispersion - strengthened tungsten
L - L	Liquid - liquid
SEM	Scanning electron microscope
S - L	Solid- liquid
TGA	Thermogravimetric analysis
XRD	X - ray diffraction

1. Introduction

Tungsten and its alloys are largely employed in the defense and nuclear industry due to their high melting point, hardness and strength at various temperatures [1-4]. It possesses a high ductile–brittle transition temperature (DBTT) with a low recrystallization temperature, which negatively influences its physical behavior [5, 6]. In order to enhance the tungsten alloys' physical behavior, the research on oxide particle dispersion - strengthened tungsten (ODS - W) alloy, is attracted more and more attentions [7-9], because these oxide particles could decrease DBTT and increase the recrystallization temperature [10-12].

With the recent progress of the powder metallurgy, the morphological and mechanical properties of particle reinforced tungsten alloys are relied on tungsten powder quality [13, 14]. High - energy ball milling of the mixed powders with pure tungsten and oxide particles is an efficient method for fabricating ultrafine doped tungsten powders. Prolonged milling time may lead to introduction of detrimental contaminants [15], inhomogeneous distribution of oxide dispersion particles and high internal stresses [16]. Solid–liquid methods were selected to obtain excellent doped tungsten powder based on the raw materials of ammonium paratungstate (APT) and soluble metal salts [11, 17]. APT powder is slightly soluble and does not react with soluble metal salts. The reaction occurs only on the surface of APT powder particles, resulting in the formation of tungsten particle aggregates [11] and the heterogeneous distribution of oxide particles [17].

Many liquid - liquid (L - L) methods were investigated to prepare the particle reinforced tungsten alloys [18-22]. The previous researches focus mainly on the tensile, compressive and torsional properties of these alloys [2]. Less research concerned the interactions of the precursor powders on the morphological properties of alloys obtained by L - L methods. Microstructural characterization of these doped ceramic particles affects the microstructural evaluation, strength and wear resistance of metal matrix composites. A. Heidarzadeh et al. [23] reported that the presence of nanoparticles increased the proportion of the continuous dynamic recrystallization compared to the discontinuous mechanism during grain structure formation. A. H. Monazzah et al. [24] indicated that intrinsic toughening had influence on the fracture resistance of composite materials based on inherent resistance of its microstructure to crack nucleation. The microstructure includes the morphology and size of reinforced phase particle. F. Xiao et al. [25] investigated the microstructure, compressive properties and wear resistance of W-ZrO_2 alloys by different preparation techniques. The results indicate that the smaller the ZrO_2 particle, the higher the compressive properties and wear resistance.

In particle strengthened composite materials, the main topics have been conducted on providing uniformly dispersed hard reinforcements in matrix [26]. These uniformly oxide particle would result in distinguished properties caused by homogenous structure, high interfacial strength and uniform deformation of composite materials [27].

The solutions with different acidities greatly influence on the reduced tungsten powders [25]. The researches concerning the effect of the solution's pH value on precursor powders, physical properties of tungsten alloys have to be studied in detail.

In this research, in order to determine the proper pH value for fabricating the uniform distribution of ultrafine oxide particle in tungsten matrix, the doped alloys fabricated with different pH values of 2, 5 and 8 were prepared. The morphologies of precursor powders were analyzed. The proper calcination process was determined through thermogravimetric analysis and differential scanning calorimetry. The

morphological, mechanical properties and abrasion resistance of alloys were studied to analyze the influence of the pH value of the solution.

This paper is structured as follows. In Section 2, the preparation process and methods of measurement and analysis of pure and doped tungsten alloy are introduced in detail. In Section 3, the morphology of precursor powders, the calcination process and the reduced powders are investigated, respectively. The microstructures of particle reinforced materials fabricated with various pH values are investigated and compared. In Section 4, the relative density, the porosity, mechanical and wear properties of the tungsten alloys are described. The main results are concluded in Section 5.

2. Experimental procedure

2.1 Materials

In the current research, different kinds of doped tungsten specimens, shown in Table 1, were elaborated via the azeotropic distillation process coupled with the powder metallurgy. The corresponding doped alloys were denoted as pH 2, pH 5 and pH 8. The commercial $Zr(NO_3)_4{\cdot}5H_2O$, $Y(NO_3)_3{\cdot}6H_2O$ and ammonium metatungstate (AMT), $(NH_4)_6H_2W_{12}O_{40}{\cdot}xH_2O$ with high - purity (99.9%) were retained as raw materials.

Table 1. The chemical composition of the tungsten alloy specimens (wt. %).

Specimens	Solution	W	ZrO_2	Y_2O_3
Pure W	2	100	0	0
pH 2	2	96.62	3.0	0.38
pH 5	5	96.62	3.0	0.38
pH 8	7	96.62	3.0	0.38

Fig. 1 illustrated the process flow diagram of tungsten alloys with the associated processing parameters. The $Y(NO_3)_3{\cdot}6H_2O$ and $Zr(NO_3)_4{\cdot}5H_2O$ solutions were mixed

under continuous stirring and heated to 90 °C until precipitates appeared. The $(NH_4)_6H_2W_{12}O_{40}{\cdot}xH_2O$ solution was added dropwise to previous solution. The pH value was measured using nitric acid or ammonia solution and stirring during 5 h at a room temperature (22 °C). The ethanol was introduced into the mixed solution as a dispersant. The mixture was continuously heated until the precursor powder appeared. The synthesized precursor powders were calcined at 550 ℃ for 4 h and reduced by following two reduction processes 750 ℃ × 2 h + 900 ℃ × 4 h under hydrogen atmosphere in order to achieve W-Zr(Y)O_2 powders.

The W-Zr(Y)O_2 powders were compressed into an elastomeric mould at the pressure of 350 MPa during 30 minutes using cold isostatic press. The cylindrical specimens were obtained with 30 mm long and a diameter of 20 mm. The specimens were sintered in an induction furnace under hydrogen atmosphere. The pre - sintering was performed at 1250 °C during 2 h. The final sintering was set at 2400 °C during 4 h.

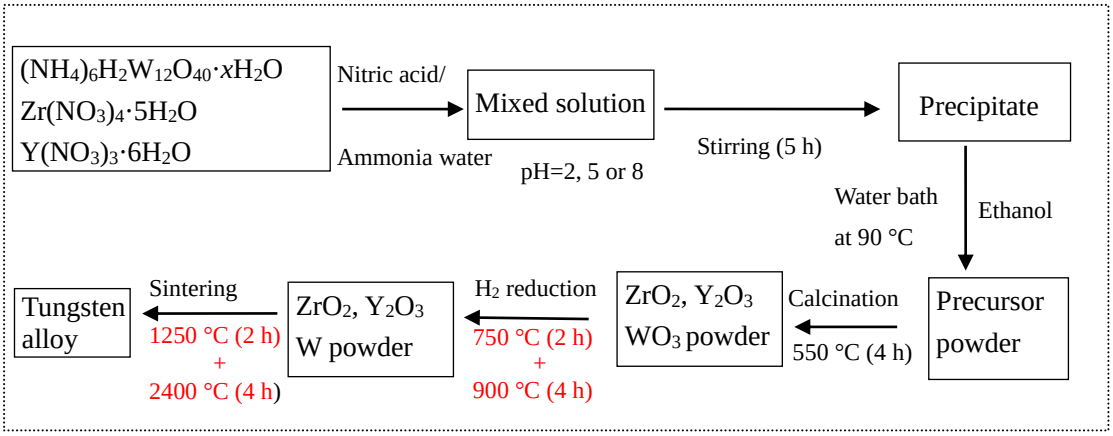

Fig. 1. Illustration of process flow diagram of tungsten alloys with the processing parameters.

2.2 Methods

The absolute density of the studied materials was determined according to ASTM B962-14 standard using Archimedes principle with ten repeated measurements in the same experimental conditions. The relative density ξ was determined by the following relation [20]:

$$\xi = \rho / \rho_0 \quad (1)$$

where ρ and ρ_0 are the absolute and theoretical density of material, respectively.

The material porosity was determined as follows:

$$P = (1 - \xi) \times 100\% \quad (2)$$

where P is the material porosity.

Vickers hardness was measured using a micro - Vickers hardness testing equipment (HVS - 1000 A) with an imposed load of 200 g for 20 s according to the ASTM E384 test method. The Vickers hardness value was an average of 10 random measurements.

Ten tests were performed using universal compression testing equipment (AG - I250 KN) at room temperature with a crosshead speed of 1.0 mm / min. Cylindrical compression specimens with a diameter and length of 6 and 10 mm.

Based on the ASTM B328 standard, the wear property was characterized using a pin - on - disc wear test (ML - 100 type). The wear test was repeated ten times. Different grit alumina waterproof - abrasive sandpapers of 240, 360, 600 and 800, respectively, were imposed with 40 N. The cylindrical specimens are: diameter 6 mm × length 20 mm. At the end of the tests, the specimens were washed with ethanol and weighted using an analytical balance.

The microstructure and chemical composition of powder and alloy specimens were analyzed by Scanning Electron Microscope (SEM, VEGA - SBH) according to the ASTM E2142-08 standard. An energy - dispersive X - ray spectrometry (EDS) was employed. The reaction of precursor powders was analyzed by using NETZSCH STA 409 PC/PG thermal analyser. Thermogravimetric analysis (TGA) was performed based on the ASTM EE228-11 standard. Differential scanning calorimeter (DSC) was effectuated according to the ASTM D3418 standard. High-resolution transmission electron microscopy (HR - TEM) was used to analyze the microstructure of the material with a Phillips FEI Titan 80–300.

3 Results and discussions

3.1 Investigation of precursor powders synthesized under various pH values

Fig. 2 shows the SEM images of powders synthesized through azeotropic distillation method corresponding to pH value of 2, 5 and 8. For pH 2, the particles possess granular structure with a size of approximately 1 - 5 μm, while several particles are with the shape of plate, as shown in Fig. 2 a). For pH 5, the microstructure of the powder is mainly in the shape of plate and block, as shown in Fig. 2 b). The length of the plate-like particle is less than 10 μm, the surface is smooth and the dispersion is well. For pH 8, the particles are mainly in the form of block with a size of 3 - 8 μm, as shown in Fig. 2 c). As a conclusion, the microstructure of the materials was significantly affected by the pH value of solution.

The particle size increases and the morphology changed greatly with the pH value of the solution. Different polytungstate species were existed in solutions with various pH values. The reaction mechanism concerning the polytungstate species with H^+ / OH^- were discussed in detail [25].

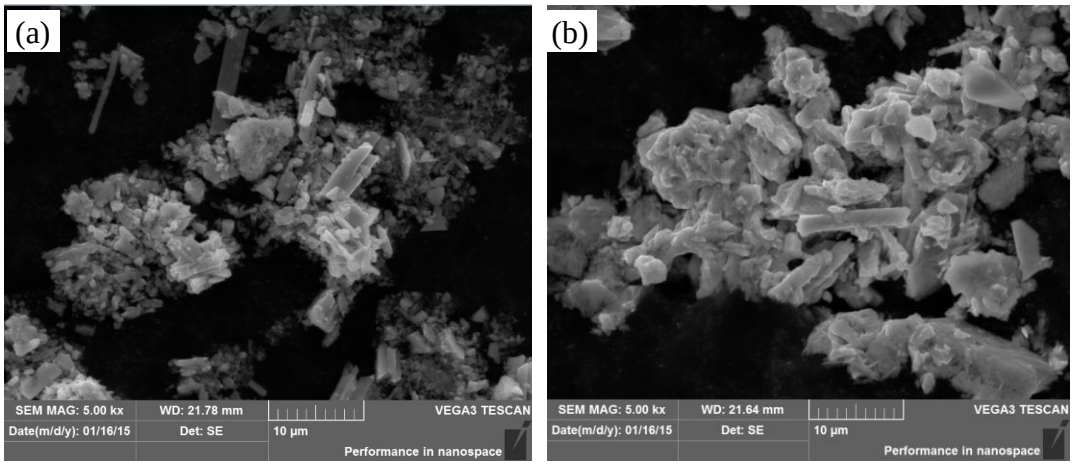

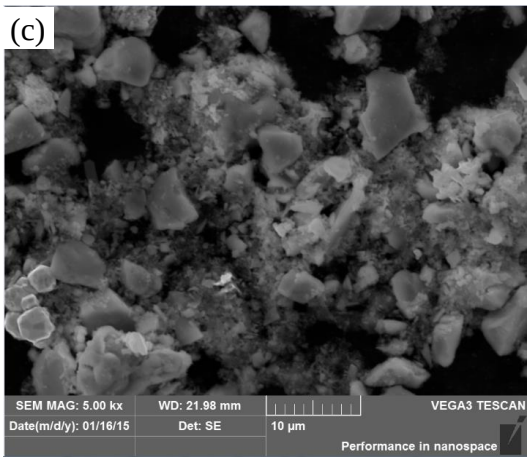

Fig. 2 SEM images of the precursor powders synthesized under: a) pH 2, b) pH 5 and, c) pH 8.

3.2 Analysis of calcined and reduced powders conducted on doped pH 2 precursor powder

The pH 2 precursor powder particle possesses finer particle structure according to the analysis in section 3.1. The TGA and DSC analyses were carried out at a heating rate of 1 °C/min in the temperature range of 20–900 °C. The calcination process was determined in an Ar atmosphere. In Fig. 3, when the temperature raised to 140 - 160 ℃, a small range of endothermic peak appeared caused by the evaporation of the adsorbed water in the material. When heated to the temperature range of about 240 ~ 340 °C with the peak at 308.3 ℃, there was an obvious exothermic peak caused by the decomposition of reaction product NH_4NO_3. Hunyadi et al. [28] described the similar phenomena that NH_3 and H_2O were released from AMT with an exothermic reaction from 240 to 340 °C. When the temperature increased to about 360 ℃, sharp endothermic peak appeared due to crystalline water loss in the reaction products.

The exothermic peak occurring at 412.7 ℃ was attributed to the transformation from WO_3 amorphous to WO_3 crystal. When the temperature increased to 550 ℃, the total weight loss of the specimens was about 7.9 %. When the temperature continued to increase, the TGA curve in Fig. 3 showed that the weight loss was almost unchanged, which indicated that the precursor powder was almost completely

decomposed at 550 ℃. The linear decrease of the total weight loss was observed in the range of 100-900°C, corresponding to the calcination process.

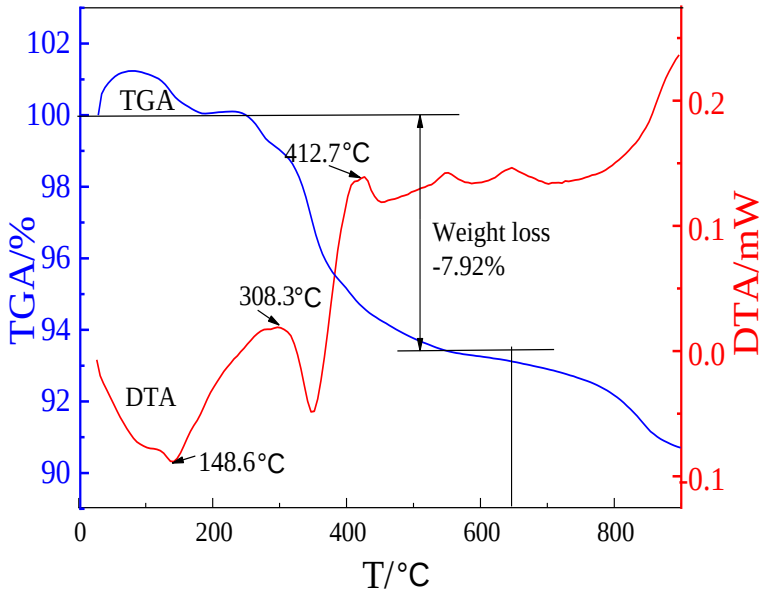

Fig. 3 TGA - DSC curves of doped precursor powder synthesized under pH 2.

The pH 2 specimens were analyzed by HR - TEM to quantify the particle morphology and phase structure. The obtained images of the powder reduced after 750 ℃×2 h + 900 ℃ × 4 h were shown in Fig 4 a). Based on Fig. 4 a), the reduced powder were regularly in a small spherical particle shape and well dispersed. The size was about 40 nm, which belonged to nano-sized particles. The selected area A corresponded to Fig. 4 b). As the nanoparticle under selected area B consisted of the containing - Zr phase and containing - Y phase through mixing these two phases firstly, the selected area B corresponded to Figs. 4 c) and, d). The reduced powder particles were calibrated with lattice fringes, as shown in Figs. 4 b), c) and d). The measured spacing of lattice fringes were 0.2460 nm, 0.3227 nm and 0.3448 nm close to the spacing of W (200), ZrO_2 (-111) and Y_2O_3 (202) crystal planes of PDF#47-1319, PDF#65-2357 and PDF#44-0399, respectively [29]. As analysis above, the reduced pH 2 powders were composed of tungsten and ZrO_2-Y_2O_3 nano-sized particles.

The formation of ZrO_2-Y_2O_3 doped powder was related to the mechanism of doped powder in the hydrogen reduction process. Y and Zr atoms were always in the

form of oxide during high - temperature reduction. Solid tungsten oxide would volatilize and then formed hydroxide $WO_2(OH)_2$ with high volatility. Hydroxide $WO_2(OH)_2$ would deposit on the surfaces of the neighbor tungsten oxide with low valence states or doped Y_2O_3-ZrO_2 particles [30]. The growth rate increase and "volatilization - deposition" would make particles full growth in the process [31, 32]. The Y_2O_3-ZrO_2 particles provided plenty of crystal nucleus, which hindered the growth of tungsten particles and eventually generated the nano-sized doped tungsten powders.

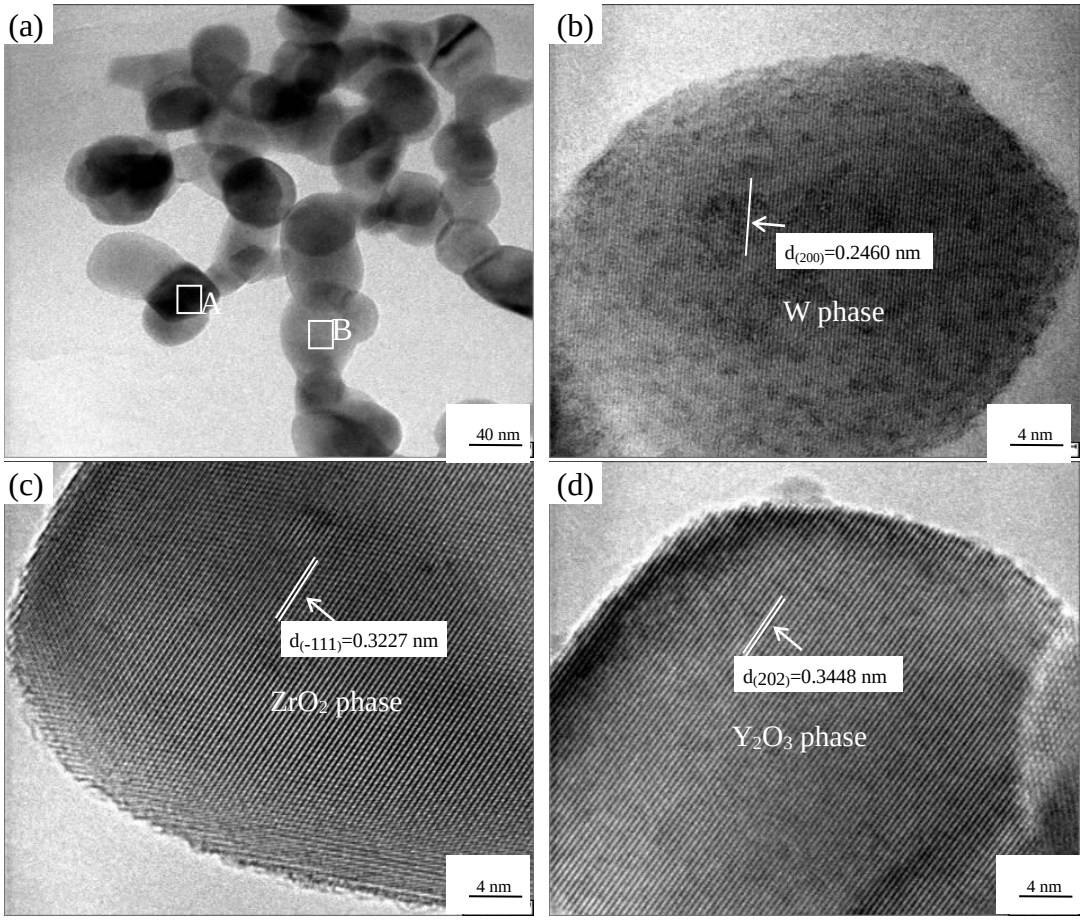

Fig. 4 HR - TEM image and diffraction fringes of reduced powders corresponding to test case pH 2 for doped W sample [29]: a) HR - TEM image of reduced powders, b) Diffraction fringes of W powder particle, c) Diffraction fringes of ZrO_2 powder particle and, (d) Diffraction fringes of Y_2O_3 powder particle.

3.3 Analysis of the microstructure of tungsten alloys

The comparison of the SEM images of pure tungsten and reinforced alloys obtained under various pH values is illustrated in Fig. 5. It shows that the grain size of pure tungsten is relatively uniform compared to the other alloys, as shown in Fig 5 a). The grain size of irregular particles is about 10 - 15 µm. Based on Figs. 5 (b - d), there are many pores among alloys mainly caused by the pressureless sintering method. The alloy density is much lower compare to the pure W. In these alloys, the grain size is in the range of 2 - 6 µm, much smaller than pure W due to the effect of grain refinement. Based on the SEM images, these particles are mostly located at W grain boundaries.

When the alloy was prepared with pH 2, the $Zr(Y)O_2$ particles were smaller in size and more uniformly distributed. In the case of pH 5, the occurrence of some bonding $Zr(Y)O_2$ particles can be observed, as marked with an arrow A. For pH 8, more and more bonding particles were observed, which was not conducive to improve the alloy properties. Based on the EDS results, the black phase is corresponding to $Zr(Y)O_2$ consisting of the elements: Zr, Y and O, as shown in Fig 5 e).

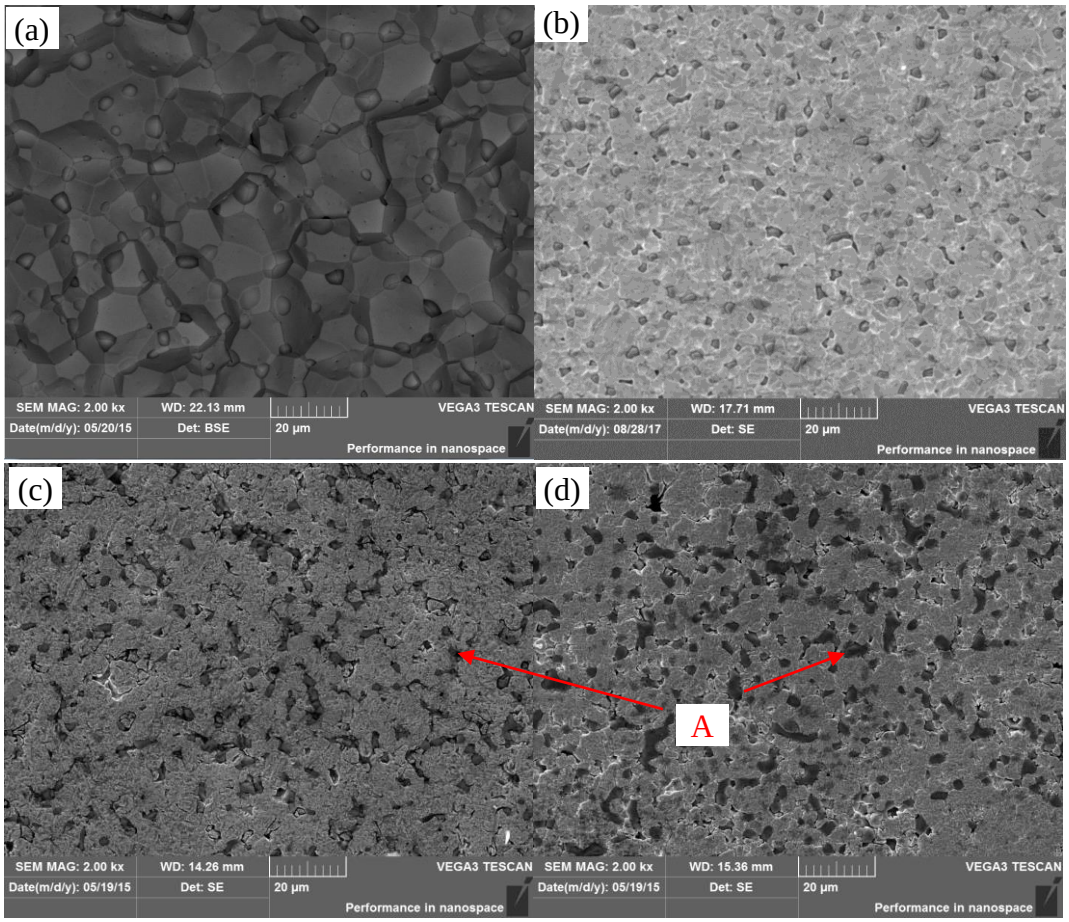

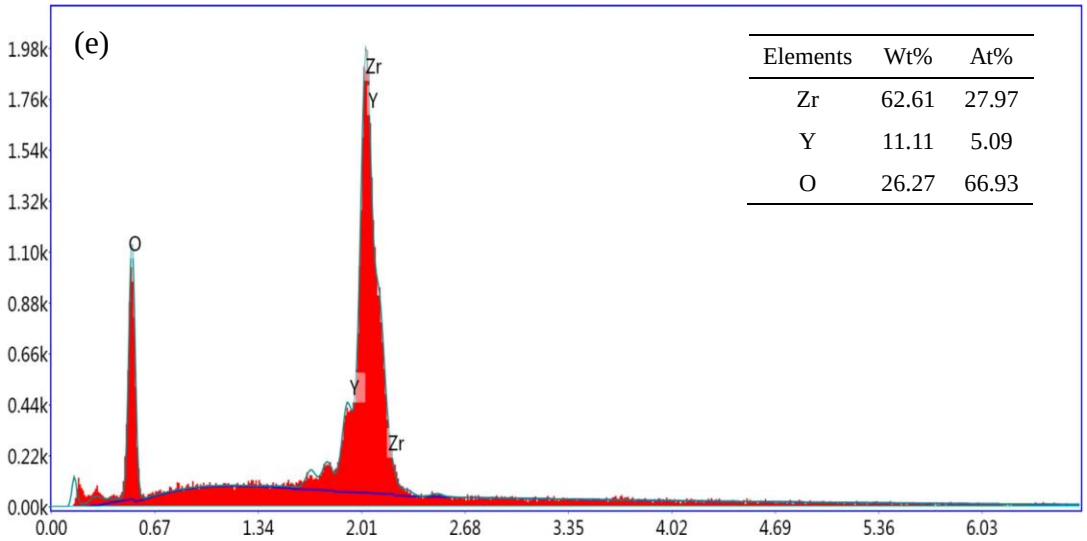

Elements	Wt%	At%
Zr	62.61	27.97
Y	11.11	5.09
O	26.27	66.93

Fig. 5 Microstructure SEM images and of EDS patterns pure and doped tungsten alloys: a) Pure W, b) pH 2, c) pH 5, d) pH 8 and, e) EDS patterns of doping phase.

XRD patterns indicate that ZrO_2 particles belong to the stabilized ZrO_2 phase, as shown in Fig. 6.

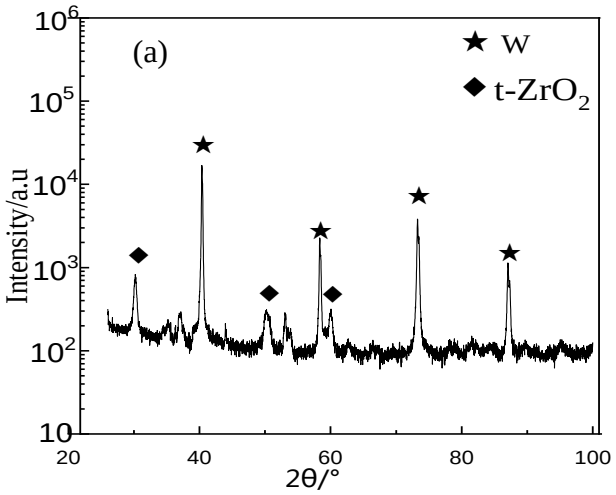

Fig. 6 XRD patterns of test case pH 2 for doped W sample.

The stabilized ZrO_2 phase among alloy was analyzed. At high temperature, stabilized zirconia with $Zr\text{-}O_8$ structure consisted of a zirconium ion and eight equidistant oxygen ions. When the temperature decreased, according to Coordination Theory, due to rZr^{4+}/rO^{2-} = 0.564 (less than 0.732), eight - coordinate structure in

ZrO_2 phase would decrease the interspace between oxygen atoms. It would lead to the increasing of the coulomb repulsion between adjacent oxygen - oxygen ions. As a result, the original crystal structure would become unstable, and then promote the transformation from stabilized structure to monoclinic structure with Zr-O_7 [33].

As shown in Fig. 7, Y^{3+} as stabilizer from Y_2O_3 particles could replace the partial Zr^{4+} atoms in ZrO_2 at high temperature, increasing the cation - anion radius ratio. Meanwhile, oxygen vacancies were introduced into the lattice to remain charge neutrality of ZrO_2 phase. It would increase the interspace of oxygen - oxygen and reduce the repulsive forces between the local oxygen - oxygen, and then promote the formation of the stability of the Zr-O_8 structure.

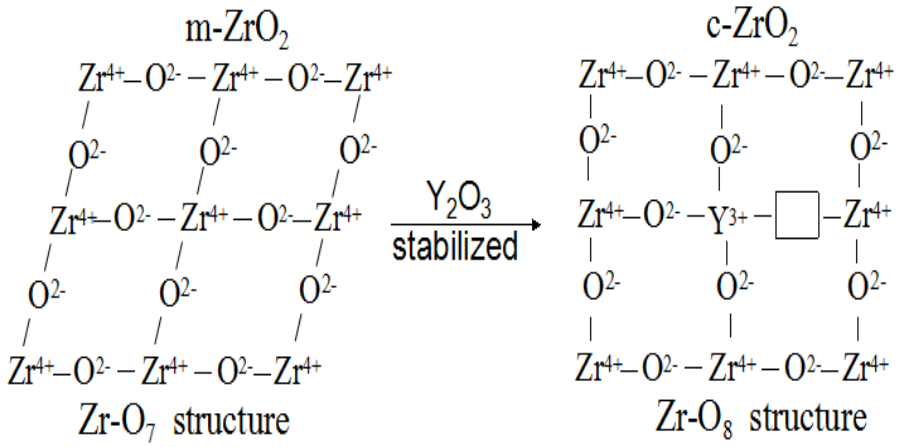

Fig. 7 Schematic flowchart of the cubic yttria - stabilized zirconia.

4. Mechanical behavior of W-Zr(Y)O_2 alloy

4.1 Compressive property

The mechanical properties of pure W and reinforced W alloys elaborated under different pH values are compared in Fig. 8. It can be seen that the pure W possesses the ultimate strain of 0.45. The ultimate strain and ultimate compressive strength value of pH 2 reach to 0.23 and 1009 MPa, respectively. For pH 2 alloy, the ultimate strain is 48.8%, lower than that of pure W (ductile behaviour). It exhibits highest strain and ultimate compressive strength value compared to pH 5 and 8 alloys. The strain and the ultimate compressive strength value of the alloy increase at lower pH values.

The enrichment zone of oxide particles was generated by the high levels of oxide particles. It resulted in the superposition of stress field round the reinforced particles [25]. It lead to the fact that weakening effect on strength in alloy was greater than the strengthening effect due to dislocation motion. It weakened the bonding strength of the W - W grain boundary and the fracture strain of W alloy.

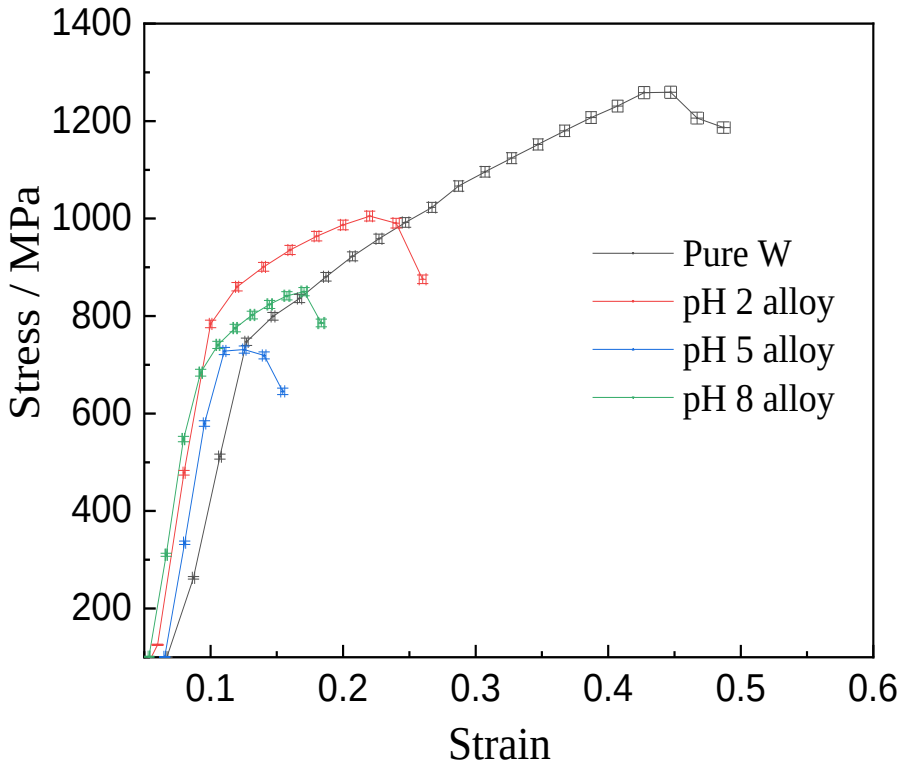

Fig. 8 Compressive stress - strain curves of tungsten alloys.

Table 2 summarizes the evolution of relative density, porosity, micro-hardness and wear resistance of the pure and doped W alloys versus pH value. The relative density of the pure W is about 97.9 %, higher compared to pH 2 alloy (i.e. 90.9 %). The micro-hardness of pH 2 alloy is lower than pure W due to the pores emerging in the sintering process. It leads to damage the metallic continuity and reduce its effective area.

The evolution of the relative density decreases with the pH value, as shown in Table 2. The associated porosity increases with the pH value. The micro-hardness of the doped alloys decreases with the pH value.

Table 2 Relative density, porosity, micro-hardness and abrasion loss of pure and doped W alloys.

Alloys	Relative density (%)	Porosity (%)	Micro-hardness (HV)	Abrasion loss (mg) [a*]
Pure tungsten	97.9 ± 0.1	2.1 ± 0.1	367 ± 15	4292 ± 100
Doped alloy (pH 2)	90.9 ± 0.1	9.1 ± 0.1	349 ± 30	3490 ± 100
Doped alloy (pH 5)	85.9 ± 0.1	14.1 ± 0.1	259 ± 26	-
Doped alloy (pH 8)	81.6 ± 0.1	18.4 ± 0.1	232 ± 35	-

a* Wear resistance test was carried out using 360 grit Al_2O_3 waterproof - abrasive sand paper under the loading of 1.40 N/mm^2.

4.2 Wear resistance

Based on the previous analysis, the pH 2 alloy exhibits better mechanical properties. In this part, the influence of zirconia content on wear resistance of pH 2 alloy is studied, summarized in Table 2.

Figs. 9 illustrates the effect of abrasive particle size on wear resistance properties of reinforced W alloys. The weight loss of the alloys decreases with the abrasive particle size of 240, 360, 600 and 800 by using the same loading of 1.40 N/mm^2. The weight loss of reinforced tungsten alloys decreases with ZrO_2 fraction from 0 to 3 wt. % with the same abrasive particles size (360 grit Al_2O_3 waterproof - abrasive). Then the weight loss of reinforced tungsten alloys increases with the ZrO_2 fraction from 3 to 10 wt. %. It proves that W-3.0%Zr(Y)O_2 alloy possesses the best wear resistance property.

The hardness of Zr(Y)O_2 particles is higher than the pure W matrix. In the abrasive wear test, the abrasive particles mainly interact with the Zr(Y)O_2 particles.

The W matrix is located in the lower wear zone, which reduces the wear loss of tungsten matrix. More internal pores in tungsten alloys are obtained with the increase of $Zr(Y)O_2$. It decreases the bonding strength between tungsten matrix and $Zr(Y)O_2$. In the test, the abrasive particles are firstly contacted with the $Zr(Y)O_2$ particles. The higher load results in the $Zr(Y)O_2$ particles falling off from the W matrix. As a result, the $Zr(Y)O_2$ and abrasive alumina particles aggravate the wear loss rate of alloy together [34].

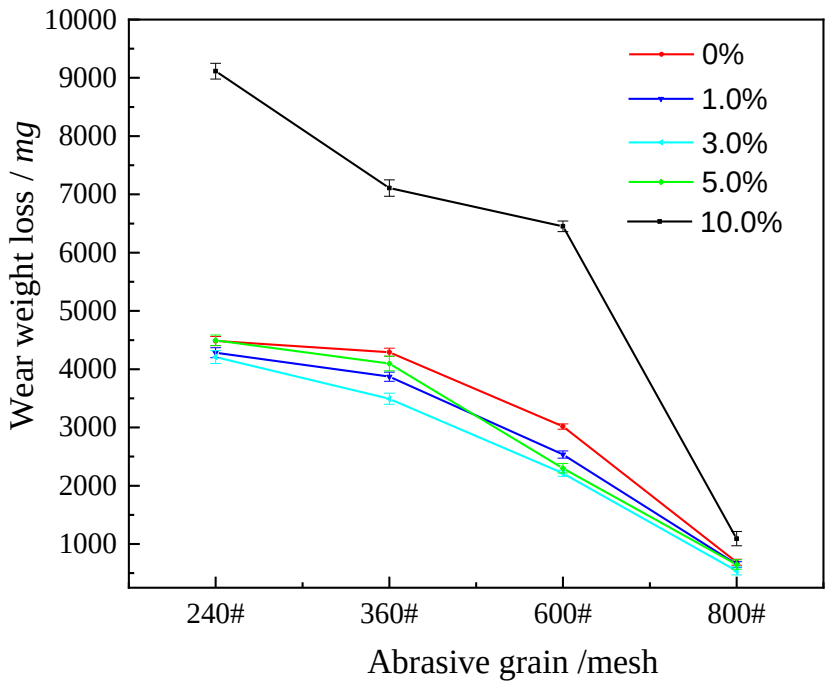

Fig. 9 Effect of abrasive particle size on the wear weight loss of W-$Zr(Y)O_2$ alloys at 1.40 N/mm^2.

5. Conclusion

1. Various precursor powders were synthesized under different pH values (2, 5 and 8). The morphological structures of the obtained powders were compared. The microstructures as well as mechanical and wear properties of the tungsten alloy elaborated with these powders were investigated.

2. The precursor' powder synthesized under solution with pH value of 2

possesses finer particles' structure. The effects of calcination process were investigated to optimize the calcination procedure through thermogravimetric analysis and differential scanning calorimetry.

3. W-Zr(Y)O_2 alloy, prepared under pH value of 2, has a better homogenous microstructure over other two alloys with pH value equal 5 and 8. It exhibits better physical and mechanical properties.

4. The effects of Zr(Y)O_2 particles content on the abrasive wear resistance of W alloy under different conditions were investigated. The abrasion mechanism was analyzed in details.

Declaration of interest

There are no conflicts to declare.

Funding: This work is supported by National Natural Science Foundation of China [No. 51672070, 51874185], and Nanjing university of aeronautics and astronautics PhD short-term visiting scholar project [No. 190107DF06].

References

[1] L. Xu, F. Xiao, S. Wei, Y. Zhou, K. Pan, X. Li, J. Li, W. Liu, Development of tungsten heavy alloy reinforced by cubic zirconia through liquid-liquid doping and mechanical alloying methods, International Journal of Refractory Metals and Hard Materials, 78 (2019): 1-8.

[2] F. Xiao, Q. Miao, S. Wei, T. Barriere, G. Cheng, S. Zuo, L. Xu, Uniform nanosized oxide particles dispersion strengthened tungsten alloy fabricated involving hydrothermal method and hot isostatic pressing, Journal of Alloys and Compounds, 824 (2020): 153894.

[3] B. Mamen, J. Song, T. Barriere, J.-C. Gelin, Experimental and numerical analysis of the particle size effect on the densification behaviour of metal injection moulded tungsten parts during sintering, Powder Technology, 270 (2015): 230-243.

[4] F. Xiao, T. Barriere, G. Cheng, Q. Miao, S. Wei, S. Zuo, Y. Yang, L. Xu, Research on the effect of liquid-liquid doping processes on the doped powders and microstructures of W–ZrO2 (Y) alloys, Journal of Alloys and Compounds, 855 (2021): 157335.

[5] N. Liu, Z. Dong, Z. Ma, L. Yu, C. Li, C. Liu, Q. Guo, Y. Liu, Eliminating bimodal structures of W-Y2O3 composite nanopowders synthesized by wet chemical method via controlling reaction conditions, Journal of Alloys and Compounds, 774 (2019): 122-128.

[6] M. Zhao, Z. Zhou, M. Zhong, J. Tan, Y. Lian, X. Liu, Thermal shock behavior of fine grained W–Y2O3 materials fabricated via two different manufacturing technologies, Journal of nuclear materials, 470 (2016): 236-243.

[7] C.-L. Chen, C.-L. Huang, Milling media and alloying effects on synthesis and characteristics of mechanically alloyed ODS heavy tungsten alloys, International Journal of Refractory Metals and Hard Materials, 44 (2014): 19-26.

[8] L. Veleva, R. Schaeublin, M. Battabyal, T. Plociski, N. Baluc, Investigation of microstructure and mechanical properties of W–Y and W–Y_2O_3 materials fabricated by powder metallurgy method, International Journal of Refractory Metals and Hard Materials, 50 (2015): 210-216.

[9] M. Qin, J. Yang, Z. Chen, P. Chen, S. Zhao, J. Cheng, P. Cao, B. Jia, G. Chen, L. Zhang, Preparation of intragranular-oxide-strengthened ultrafine-grained tungsten via low-temperature pressureless sintering, Materials Science and Engineering: A, 774 (2020): 138878.

[10] P. Senapati, B. Mishra, A. Parida, Modeling of viscosity for power plant ash slurry at higher concentrations: Effect of solids volume fraction, particle size and hydrodynamic interactions, Powder Technology, 197 (2010): 1-8.

[11] M. A. Yar, S. Wahlberg, H. Bergqvist, H. G. Salem, M. Johnsson, M. Muhammed, Chemically produced nanostructured ODS–lanthanum oxide–tungsten composites sintered by spark plasma, Journal of nuclear materials, 408 (2011): 129-135.

[12] Z. Chen, M. Qin, J. Yang, L. Zhang, B. Jia, X. Qu, Effect of La2O3 addition on the synthesis of tungsten nanopowder via combustion-based method, Journal of Materials Science & Technology, 58 (2020): 24-33.

[13] F. Xiao, T. Barriere, G. Cheng, Q. Miao, S. Wei, S. Zuo, Z. Huang, L. Xu, Research on preparation process for the in situ nanosized Zr (Y) O2 particles dispersion-strengthened tungsten alloy through synthesizing doped hexagonal (NH4) 0.33· WO3, Journal of Alloys and Compounds, 843 (2020): 156059.

[14] Y. Liang, Z. Wu, E. Fu, J. Du, P. Wang, Y. Zhao, Y. Qiu, Z. Hu, Refinement process and mechanisms of tungsten powder by high energy ball milling, International Journal of Refractory Metals and Hard Materials, 67 (2017): 1-8.

[15] U. R. Kiran, M. P. Kumar, M. Sankaranarayana, A. Singh, T. Nandy, High energy milling on tungsten powders, International Journal of Refractory Metals and Hard Materials, 48 (2015): 74-81.

[16] Z. Dong, N. Liu, Z. Ma, C. Liu, Q. Guo, Y. Yamauchi, H. R. Alamri, Z. A. Alothman, M. S. A. Hossain, Y. Liu, Synthesis of nanosized composite powders via a wet chemical process for sintering high performance W-Y2O3 alloy, International Journal of Refractory Metals and Hard Materials, 69 (2017): 266-272.

[17] M. A. Yar, S. Wahlberg, H. Bergqvist, H. G. Salem, M. Johnsson, M. Muhammed, Spark plasma sintering of tungsten–yttrium oxide composites from chemically synthesized nanopowders and microstructural characterization, Journal of nuclear materials, 412 (2011): 227-232.

[18] F. Xiao, L. Xu, Y. Zhou, K. Pan, J. Li, W. Liu,S. Wei, A hybrid microstructure design strategy achieving W-ZrO2 (Y) alloy with high compressive strength and critical failure strain, Journal of Alloys and Compounds, 708 (2017): 202-212.

[19] C. Yuntao, W. Jinshu, L. Wei, W. Xi, Effect of scandia on tungsten oxide powder reduction process, Journal of Rare Earths, 28 (2010): 202-205.
[20] F. Xiao, L. Xu, Y. Zhou, K. Pan, J. Li, W. Liu, S. Wei, Preparation, microstructure, and properties of tungsten alloys reinforced by ZrO2 particles, International Journal of Refractory Metals and Hard Materials, 64 (2017): 40-46.
[21] Y. Han, J. Fan, T. Liu, H. Cheng, J. Tian, The effect of trace nickel additive and ball milling treatment on the near-full densification behavior of ultrafine tungsten powder, International Journal of Refractory Metals and Hard Materials, 34 (2012): 18-26.
[22] H. Wen, T. Dunqiang, L. Yalei, Y. Xin, L. Lei, L. Deping, Effect of rare earth element cerium on preparation of tungsten powders, Journal of Rare Earths, 33 (2015): 561-566.
[23] A. Heidarzadeh, H. Pouraliakbar, S. Mahdavi, M. R. Jandaghi, Ceramic nanoparticles addition in pure copper plate: FSP approach, microstructure evolution and texture study using EBSD, Ceramics International, 44 (2018): 3128-3133.
[24] A. H. Monazzah, R. Bagheri, S. S. Reihani, H. Pouraliakbar, Toughness enhancement in architecturally modified Al6061-5 vol.% SiCp laminated composites, International Journal of Damage Mechanics, 24 (2015): 245-262.
[25] F. Xiao, Q. Miao, S. Wei, Z. Li, T. Sun, L. Xu, Microstructure and mechanical properties of W-ZrO2 alloys by different preparation techniques, Journal of Alloys and Compounds, 774 (2019): 210-221.
[26] H. Pouraliakbar, A. Nazari, P. Fataei, A. K. Livary, M. Jandaghi, Predicting Charpy impact energy of Al6061/SiCp laminated nanocomposites in crack divider and crack arrester forms, Ceramics International, 39 (2013): 6099-6106.
[27] A. H. Monazzah, H. Pouraliakbar, R. Bagheri, S. S. Reihani, Toughness behavior in roll-bonded laminates based on AA6061/SiCp composites, Materials Science and Engineering: A, 598 (2014): 162-173.
[28] D. Hunyadi, I. Sajó, I. M. Szilágyi, Structure and thermal decomposition of ammonium metatungstate, Journal of Thermal Analysis and Calorimetry, 116 (2014): 329-337.
[29] F. Xiao, Q. Miao, T. Barriere, G. Cheng, S. Zuo, L. Xu, A study on the effect of solution acidity on the microstructure, mechanical, and wear properties of tungsten alloys reinforced by yttria-stabilised zirconia particles, Materials Today Communications, (2021): 102223.
[30] F. Xiao, Q. Miao, S. Wei, W. Liang, X. Fan, K. Pan, L. Xu, Hydrothermal synthesis of nanoplates assembled hierarchical h-WO3 microspheres and phase evolution in preparing cubic Zr (Y) O2-doped tungsten powders, Advanced Powder Technology, 29 (2018): 2633-2643.
[31] T. Zimmerl, W.-D. Schubert, A. Bicherl, A. Bock, Hydrogen reduction of tungsten oxides: Alkali additions, their effect on the metal nucleation process and potassium bronzes under equilibrium conditions, International Journal of Refractory Metals and Hard Materials, 62 (2017): 87-96.
[32] Y. Hua, J. Wang, J. Ma, S. Chen, C. Lai, D. den Englsen, Effect of yttrium doping on the formation and stability of β-tungsten powder, International Journal of Refractory Metals and Hard Materials, 72 (2018): 71-77.
[33] Z. Xie, R. Liu, T. Zhang, Q. Fang, C. Liu, X. Liu, G. Luo, Achieving high strength/ductility in bulk W-Zr-Y2O3 alloy plate with hybrid microstructure, Materials & Design, 107 (2016): 144-152.

[34] S. Wei, L. Xu, Review on research progress of steel and iron wear-resistant materials, Acta Metall Sin, 56 (2019): 523-538.